

THE COMPLEX BROAD-BAND X-RAY SPECTRUM  
OF THE STARBURST GALAXY M82

EDWARD C. MORAN & MATTHEW D. LEHNERT<sup>1</sup>

Institute of Geophysics and Planetary Physics  
Lawrence Livermore National Laboratory  
Livermore, CA 94550

ABSTRACT

The broad-band X-ray spectrum of the prototypical starburst galaxy M82 is very complex. At least three spectral components are required to fit the combined *ROSAT* and *ASCA* spectrum in the 0.1–10 keV range. The observed X-ray flux in this band is dominated by a hard  $\Gamma = 1.7$ , heavily absorbed power law component which originates in the nucleus and near-nuclear disk of the galaxy. Among the candidates for the origin of this hard X-ray emission, the most plausible appears to be inverse-Compton scattered emission from the interaction of M82's copious infrared photon flux with supernova-generated relativistic electrons. The measured intrinsic luminosity of the power law component agrees closely with calculations of the expected inverse-Compton luminosity. Moreover, the radio and X-ray emission in the nucleus of M82 have the same spectral slope, which should be the case if both types of emission are nonthermal and are associated with a common population of electrons. The other two spectral components, thermal plasmas with characteristic temperatures  $kT \approx 0.6$  and 0.3 keV, are associated with the star formation and starburst-driven wind in M82. The warmer thermal component is heavily absorbed as well and must also originate in the central region of the galaxy. The softer thermal component, however, is not absorbed, and is likely to represent the X-ray emission that extends along M82's minor axis. The amount of absorption required in the three-component model suggests that the intrinsic luminosity of M82 in the 0.1–10 keV band is about four times greater than its observed luminosity of  $4 \times 10^{40}$  ergs s<sup>-1</sup>.

*Subject headings:* galaxies: individual (M82) — galaxies: starburst — X-rays: galaxies

---

<sup>1</sup> Present Address: Sterrewacht Leiden, Postbus 9513, 2300 RA Leiden, The Netherlands

## 1. INTRODUCTION

Several different sources of X-rays have been identified as contributors to the total X-ray emission from star-forming galaxies, including stars, accreting binary star systems, supernova remnants, diffuse hot phases of the interstellar medium, and outflowing “winds” (Fabbiano 1989). Since the radiative processes and/or physical conditions associated with these sources differ considerably, X-ray spectroscopy should, in principle, reveal the relative importance of each emission component and afford us a better understanding of the violent processes occurring within starburst galaxies. But X-ray observations of star-forming galaxies have not yet provided a definitive picture of their high-energy properties. Starburst galaxies are not particularly luminous X-ray sources; thus, detailed information has been available for only the closest, highest flux objects. Moreover, spectra of the best-studied galaxies have been difficult to interpret because of differences and limitations in the sensitivity, spectral resolution, and energy range of the instruments used to acquire them. The nearby starburst galaxy M82 (= NGC 3034), for example, has been observed with every major X-ray mission flown over the past 15 years. But, as summarized in Table 1, the spectra obtained have yielded a wide variety of models for the galaxy’s integrated X-ray emission.

The *ROSAT* and *ASCA* observatories, with comparable sensitivity and spectral resolution over a combined bandpass of 0.1–10 keV, offer a possible remedy to the situation. In this study, we present the analysis of high signal-to-noise X-ray spectra of M82 obtained from long exposures with both observatories. Our objective is to ascertain a comprehensive model for M82’s broad-band X-ray spectrum and, with use of the spatial information provided in the *ROSAT* image, determine the physical origins of its different components. These results, in addition to providing new insight into the nature of the starburst in M82, will aid the interpretation of *ROSAT* and *ASCA* observations of more distant starburst galaxies, which are likely to be far inferior to those presented herein.

## 2. X-RAY OBSERVATIONS AND DATA REDUCTION

Observations of M82 with the *Einstein Observatory* provided clear evidence that the X-ray emission from M82 is very extended (Watson, Stanger, & Griffiths 1984; Fabbiano 1988). Unfortunately, the imaging capabilities of the optics employed on *ASCA* provide only limited information about the spatially resolved emission. Therefore, this investigation focuses primarily on the integrated spectrum of M82, although we will draw upon spatial information contained in the *ROSAT* image to interpret the results of our spectral fits.

The *ROSAT* and *ASCA* X-ray data for M82 were acquired from the HEASARC archive at NASA Goddard Space Flight Center (GSFC). M82 was observed with the *ROSAT* Position Sensitive Proportional Counter (PSPC) in the 0.1–2.4 keV energy band for a total of 26.1 ksec on 28 March and 16 October 1991. *ASCA* observed M82 on 19–20 April 1993 for 27.8 ksec in the 0.6–10 keV range with the two moderate-resolution Gas Imaging Spectrometers, GIS2 and GIS3. In the 0.4–10 keV band, exposures totaling 16.7 ksec and 15.7 ksec were obtained with *ASCA*’s high-resolution Solid-state Imaging Spectrometers SIS0 and SIS1, respectively. The photon event files for all five data sets were filtered using the standard procedures for each instrument to ensure that we have included only the cleanest data. For example, we rejected *ASCA* data collected during periods of enhanced

background, such as those that result from passages of the observatory through the South Atlantic Anomaly. Data collected at times when the geomagnetic cut-off rigidity was low (below  $6 \text{ GeV } c^{-1}$ ) and when the telescope optical axes were close to the Earth’s limb (within  $5^\circ$  for the GIS or  $20^\circ$  for the SIS) were also filtered out. “Light curves” for each observation were examined to certify that no high-background data remained.

Consistent with previously published X-ray images of M82 (Watson *et al.* 1984; Fabiano 1988; Bregman, Schulman, & Tomisaka 1995), the PSPC image indicates that M82’s soft X-ray emission extends mainly along its minor axis (Fig. 1). Therefore, we collected PSPC source counts within an elliptical region oriented at  $\text{PA} = 140^\circ$  with semimajor and semiminor axes of  $8'$  and  $4.5'$ , respectively. We estimated the background contribution by extracting counts from  $3'$ -wide annular arcs (free of bright background point sources) located outside the source region to the southwest and northeast of the galaxy. Subtraction of the background (10% of the total source-region counts) produced a PSPC spectrum with 31,180 counts.

In the GIS fields, source counts were extracted from circular regions  $8'$  in radius centered on the nucleus of M82. Background counts were collected in  $3'$ -wide annular arcs positioned approximately the same distance off-axis as the bulk of the emission from M82, in order to minimize the effects of vignetting on the background measurement. Background accounts for 7.5% of the counts in the source region. The GIS2 and GIS3 spectra of M82 contain 16,499 and 16,920 background-subtracted counts, respectively.

The SIS instruments were operated in 4-CCD mode. We collected SIS source counts from pixels on all four chips within  $8'$  of the center of the galaxy. We then extracted background counts from identical regions in similarly filtered SIS “blank sky” images, provided by GSFC. Background contributes very little to the SIS spectra (just 2.2% for SIS0 and 2.8% for SIS1). The total number of background-subtracted counts is 16,222 and 12,125 for the SIS0 and SIS1 spectra, respectively. The substantially lower number of SIS1 counts has several causes: (1) less good exposure time was obtained with SIS1; (2) the source in the SIS1 observation was further off-axis, and thus more vignetted; (3) the source in the SIS1 observation was positioned closer to the edge of the CCD, so relatively more counts were lost down the gaps between the chips.

The PSPC, GIS, and SIS spectra were rebinned to provide a minimum of 150, 100, and 50 counts per energy channel, respectively, ensuring that  $\chi^2$  will be a meaningful statistic for goodness-of-fit.

### 3. MODELING M82’S 0.1–10 KILOVOLT X-RAY SPECTRUM

Our primary objective in this study is to characterize the spectrum of M82 over the widest possible energy range; thus, we have analyzed the *ROSAT* and *ASCA* spectra simultaneously. We have elected to consider first the combined PSPC/GIS spectrum in order to obtain a low-resolution overview of the broad-band X-ray properties of M82. The energy resolution of the GIS is well-matched to that of the PSPC, so the data over the entire 0.1–10 keV bandpass are comparably sensitive to the details of models we apply. These results provide a useful framework within which to interpret the significantly more detailed SIS spectrum.

### 3.1. Low-Resolution PSPC/GIS Spectral Fits

Separate analyses of the PSPC and GIS spectra of M82 give very discrepant results, primarily due to the different bandpass limits of each instrument. A simultaneous fit to these spectra, therefore, is necessary to characterize spectral features at both the high- and low-energy extremes of the 0.1–10 keV range. Using the XSPEC software, we have applied a variety of models to the combined PSPC/GIS spectrum, each consisting of one to three spectral components. The results of the fits are summarized in Table 2. To allow for differences in the absolute calibration of each instrument, we permitted the model normalizations for all three data sets to be independent parameters in the fits.

Based on differences in the single-temperature thermal models derived from the *Einstein* IPC and MPC spectra of M82, Fabbiano (1988) suggested that the broad-band spectrum of M82 may be intrinsically complex. The high values of  $\chi^2$  obtained for the single-component fits to the PSPC/GIS spectrum, thermal or nonthermal, immediately rule out such simple models and confirm Fabbiano’s speculation. It is important to note, however, that the best-fit parameters we find for single-component models are similar to some of the results obtained previously with other instruments (*cf.* Table 1). Nonetheless, there is no question that a more complex model is required.

The presence of a very conspicuous emission line near 1.9 keV in the GIS spectra (corresponding to Si XIII and Si XIV) suggests that at least one of the components in a multiple-component fit should be an optically thin thermal plasma (Raymond-Smith plasma, hereafter R-S). Thus, we have tried two-component models involving a thermal bremsstrahlung (TB) or power law (PL) in combination with a R-S. (Heavy element abundances in all R-S components we employ are assumed to be solar.) A similar two-component model was used by Petre (1992) to fit the BBXRT spectrum of M82. A substantial reduction in  $\chi^2$  is achieved with the addition of the second component; the resultant  $\chi_\nu^2$  ( $= \chi^2/\nu$ , where  $\nu$  is the number of degrees of freedom) is about 1.3. The “hard” (PL or TB) component is very hard indeed, with an associated photon index  $\Gamma \approx 1.6$  or temperature  $kT \approx 15$  keV. The “warm” R-S component has a temperature  $kT \approx 0.6$  keV. Note, however, that the best-fit absorption column density required for the warm component ( $N_{\text{H}} = 2.5\text{--}3.6 \times 10^{20} \text{ cm}^{-2}$ ) is well below the value of the Galactic neutral hydrogen column density in the direction of M82 of  $N_{\text{H}} = 4.5 \times 10^{20} \text{ cm}^{-2}$  (Stark *et al.* 1992). Furthermore, the fit, displayed in Figure 2a with the PSPC/GIS spectra, does a very poor job in the vicinity of the silicon lines.

To better fit the emission lines, we added a third component—a second R-S plasma—to the model. Once again, the overall fit improves significantly with the additional component:  $\chi^2$  decreases by more than 100. Interestingly, the spectral parameters for the original two components are virtually unchanged: for the hard component,  $\Gamma = 1.7$  (or,  $kT = 18$  keV), and for the warm component,  $kT = 0.5\text{--}0.6$  keV. The third component is very soft, with a temperature  $kT \approx 0.3$  keV. What has changed in the three-component fit is the degree to which each component is absorbed. The hard and warm components are both absorbed by large columns ( $\sim 10^{22} \text{ cm}^{-2}$ ). The very soft component, on the other hand, is absorbed by a column just equal to the Galactic value. The PSPC/GIS spectrum with the three-component fit is displayed in Figure 2b. Comparison of Figure 2b to the two-component fit shown in Figure 2a illustrates clearly the higher quality of the three-component fit, which alone justifies adoption of the more complex model. We present additional evidence in § 4.1 which supports the three-component model in detail.

The PSPC and GIS3 spectra and the three-component model (with the instrument responses unfolded) are displayed in Figure 3 to illustrate the relative contribution of each component to the total X-ray emission from M82. In this model, the total X-ray flux in the 0.3–10 keV band is  $F_X = 3.2 \times 10^{-11}$  ergs cm $^{-2}$  s $^{-1}$ , which, at an assumed distance of 3.25 Mpc (Tammann & Sandage 1968), corresponds to a luminosity of  $L_X = 4.0 \times 10^{40}$  ergs s $^{-1}$ . The *unabsorbed* flux and luminosity in the same band are four times greater than the observed values:  $F_X = 1.3 \times 10^{-10}$  ergs cm $^{-2}$  s $^{-1}$  and  $L_X = 1.6 \times 10^{41}$  ergs s $^{-1}$ . The observed fraction of flux contained in each of the hard, warm, and soft components is 0.68, 0.24, and 0.08, respectively. In the absence of absorption, these fractions would be 0.24, 0.73, and 0.03.

### 3.2. The High-Resolution SIS Spectrum

The ASCA SIS, with higher spectral resolution and greater low-energy sensitivity than the GIS, should offer further insight into the X-ray properties of M82. But as Table 3 indicates, none of the model types considered in the PSPC/GIS analysis provides a statistically acceptable fit to the SIS spectrum. The best fit is obtained with a three-component model similar to the one determined in the previous section, but the fit is extremely poor ( $\chi^2 = 1.78$ ). However, as illustrated in Figure 4, the discrepancy between the three-component model and data near the emission lines in M82’s spectrum dominates the contribution to  $\chi^2$ . The poor SIS fit, therefore, is *not* an indication that the three-component model is incorrect; instead, it reveals that R-S plasmas, which assume ionization equilibrium, do not adequately describe M82’s emission-line gas at the resolution of the SIS. The inclusion of additional thermal components or nonsolar heavy element abundances does not improve the SIS fit significantly. Thus, nonequilibrium ionization conditions in the hot gas, rather than multiple gas temperatures or enhanced abundances, are likely to be responsible (Shull 1982). Differences in the “best fit” spectral parameters obtained in the SIS and PSPC/GIS fits are primarily artifacts of the  $\chi^2$  minimization fitting procedure. For this reason, the exact temperatures and abundances of the thermally emitting gas derived using R-S components, which are clearly inappropriate, should be considered uncertain (see Shull 1982).

The SIS and GIS data can be used in combination to evaluate the shape of M82’s hard X-ray spectrum, which is unaffected by absorption and uncontaminated by the soft thermal components above  $\sim 5$  keV (see Fig. 3), independent of the other details of the three-component model. A power-law fit to all four spectra in the 5–10 keV band yields a photon index  $\Gamma = 1.70 \pm 0.16$  (90% confidence for one interesting parameter).

## 4. THE ORIGIN OF X-RAYS IN M82

### 4.1. The Nature of the Hard Spectral Component

The heavy absorption of the hard X-ray component found in the fit to the PSPC/GIS spectrum of M82 implies that this component is associated with the nuclear region of the galaxy, which was found to be more absorbed than surrounding regions in the *Einstein* IPC study of M82 (Fabbiano 1988). To confirm this association, we constructed a simple X-ray “hardness map” from the PSPC image, which, despite its limited energy range, provides insight into the spatial dependence of M82’s spectral properties. The hardness

map was made by dividing the hard-band (1.0–2.4 keV) PSPC image by the soft-band (0.1–1.0 keV) PSPC image. The demarcation energy of 1 keV was chosen because the hard spectral component dominates the emission above  $\sim 1$  keV in the three-component model. The hardness map, displayed in Figure 5, clearly illustrates that the hardest X-ray flux is emitted in the nucleus and near-nuclear disk of M82, and that the emission extended along the galaxy’s minor axis is comparatively much softer. The hard spectral component, therefore, must originate mainly in the nuclear region.

The hardness map also qualitatively confirms the degree to which the hard spectral component is absorbed in the three-component model. In the nucleus of M82, the hardness map indicates that counts in the hard band outnumber those in the soft band by as much as a factor of 4. In the three-component model, hard-to-soft counts ratios in excess of 4 are possible, even with a considerable contribution by the  $\sim 0.5$  keV thermal component. Models lacking significant absorption of the hard spectral component simply cannot produce hard-to-soft counts ratios this high. For example, in the two-component models discussed in § 3.1, the maximum possible ratio of hard to soft counts is just 1.7, even if *all* of the nuclear emission is attributed to the hard component.

Thus, the following picture has emerged: most of the X-rays from M82 with energies in excess of  $\sim 1$  keV originate from the near-nuclear region of the galaxy; they are associated with a hard, highly absorbed ( $N_{\text{H}} > 10^{22} \text{ cm}^{-2}$ ) component that is well fitted by a power law with a photon index  $\Gamma \approx 1.7$  or, equivalently, with a  $\sim 18$  keV bremsstrahlung model. This emission could arise from a number of possible sources, including a buried active nucleus, an extremely hot, diffuse gas, an ensemble of X-ray binary systems, or inverse-Compton scattered radiation. In this section, we examine the case for each of these possibilities.

#### 4.1.1. A Buried Active Nucleus?

The nuclear activity in M82, based on observations across the entire electromagnetic spectrum, has always been attributed to a vigorous burst of star formation. M82’s optical spectrum is unambiguously H II region-like (e.g., Kennicutt 1992), its discrete nuclear radio sources are spatially resolved, suggesting that they are supernova remnants (Muxlow *et al.* 1994), and its nuclear X-ray emission is extended (Watson *et al.* 1984; Bregman *et al.* 1995). By contrast, the neighboring galaxy M81, which has an X-ray luminosity nearly identical to that of M82, possesses all the attributes of an active galactic nucleus (AGN): a broad emission-line optical spectrum (Peimbert & Torres-Peimbert 1981), a compact, inverted-spectrum nuclear radio source (Bartel *et al.* 1982), and a point-like nuclear X-ray source (Elvis & Van Speybroeck 1982). Nonetheless, the hard  $\Gamma \approx 1.7$  X-ray power-law spectrum we find for M82 is suspiciously similar to the canonical Seyfert galaxy X-ray spectrum (e.g., Nandra & Pounds 1994). For this reason, we would like to consider the possibility that M82 harbors a buried active nucleus.

Although we cannot isolate M82’s nuclear X-ray source spatially in the *ASCA* images, the combined results of the PSPC/GIS spectral fitting (Fig. 3) and the PSPC hardness map (Fig. 5) suggest that it can be isolated *spectrally* by considering the galaxy’s emission in the 3.5–10 keV band. A light curve of the GIS data in this energy range, displayed in Figure 6, indicates that M82’s nuclear X-ray source is not significantly variable on timescales of minutes or hours, as some Seyfert galaxies are known to be (see Matsuoka *et al.* 1990).

Measurement of M82’s hard X-ray spectrum allows us to investigate whether or not a buried active nucleus in the galaxy would be detectable at optical wavelengths. In Seyfert

galaxies, a strong correlation between the 2–10 keV X-ray luminosity and the broad H $\alpha$  emission-line luminosity has been established ( $L_X/L_{H\alpha} \approx 40$ ; Elvis, Soltan, & Keel 1984). The correlation holds for the lowest luminosity Seyfert galaxies as well (Koratkar *et al.* 1995), including M81. Thus, we can use the measured hard X-ray luminosity of M82 to estimate the strength of the H $\alpha$  line expected if the X-rays are produced by an active nucleus. The unabsorbed 2–10 keV luminosity of M82 is  $3 \times 10^{40}$  ergs s $^{-1}$ , which predicts a broad H $\alpha$  line flux of  $6 \times 10^{-13}$  ergs cm $^{-2}$  s $^{-1}$ . Assuming, however, that the emission line photons pass through the same absorbing column as the hard X-rays, (*i.e.*,  $N_H \approx 10^{22}$  cm $^{-2}$ , equivalent to 5 magnitudes of extinction at H $\alpha$ ; Zombeck 1990), the observed H $\alpha$  flux would be less by a factor of 100. In Figure 7 we have overlaid a broad H $\alpha$  line of the expected intensity on an optical spectrum of M82’s nucleus. We have fixed the velocity width of the line at 3000 km s $^{-1}$  full-width at half-maximum, similar to H $\alpha$  linewidths in other low-luminosity Seyfert galaxies (Koratkar *et al.* 1995). Figure 7 clearly illustrates that the broad H $\alpha$  emission associated with an active nucleus would be detectable if such a nucleus were present in M82.

Rieke *et al.* (1980) have estimated the visual extinction toward the nucleus of M82 to be in excess of 25 magnitudes, far greater than the  $\sim 5$  magnitudes implied by the absorption of the hard X-ray component. This discrepancy could be due to an enhancement of the dust-to-gas ratio in M82, which, if present, would mean that we have overestimated the broad H $\alpha$  flux expected from a buried AGN. Alternatively, the discrepancy between the visual and X-ray extinction might suggest that the hard X-ray emission is not produced by a compact source in the nucleus of M82, but is extended about the central region of the galaxy. The extended appearance of the hard X-ray source in the PSPC hardness map (Fig. 5) supports this speculation.

Thus, despite the spectral similarity between M82 and a typical AGN, all other aspects of the galaxy’s nuclear emission, at any wavelength, fail to confirm the presence of a buried Seyfert nucleus. We must therefore look to the starburst itself for the source of M82’s hard X-ray emission.

#### 4.1.2. Hot, Diffuse Gas?

The extended X-ray halo of M82 has been interpreted as emission from hot gas since its discovery (Watson *et al.* 1984). Based on the *Einstein* IPC spectrum, Fabbiano (1988) suggested that M82’s nuclear X-ray emission may also be thermal in nature. As discussed in the previous section, M82’s hard X-ray source is probably distributed throughout the nuclear region. Furthermore, we have found that a bremsstrahlung component models the hard X-ray emission as well as a power law does, so hot gas cannot be ruled out on spectral grounds. However, the strong 6.7 keV Fe K $\alpha$  line *expected* to accompany the thermal emission from a  $\sim 18$  keV gas is not observed in the *ASCA* spectra. A R-S fit to the four-instrument *ASCA* spectrum in the 4–10 keV range indicates that the line, if present, must be very weak, and places an upper limit to the heavy element abundance of a gas at 0.3 solar (90% confidence). Hot gas near the starburst nucleus of M82, composed of supernova ejecta and swept-up interstellar material, is not likely to be this metal-poor (see Puxley *et al.* 1989).

#### 4.1.3. X-Ray Binaries?

By analogy to the Milky Way and other Local Group galaxies, X-ray binary systems are expected to make an important contribution to the total X-ray emission of star-forming

galaxies (Fabbiano 1989). *ROSAT* HRI observations have indicated that there are at least a few point-like X-ray sources in M82 (Bregman *et al.* 1995). But if X-ray binaries are to play a significant role in M82, they must demonstrate the appropriate spectral characteristics. Low-mass X-ray binaries, with fairly soft X-ray spectra (White *et al.* 1986) and long evolutionary timescales ( $\sim 10^9$  yr) relative to the age of the starburst in M82 ( $10^7$ – $10^8$  yr; Rieke *et al.* 1980; Bernlöhr 1993), cannot be responsible for the majority of M82’s hard X-rays. The spectra of high-mass X-ray binaries, on the other hand, are typically too hard ( $\Gamma = 0.8$ – $1.5$  below 10 keV; Nagase 1989) to be compatible with M82’s X-ray spectrum; they, too, are unlikely to produce M82’s hard X-ray emission. The black hole candidate Cyg X-1, however, possesses a low-state X-ray spectrum nearly identical to that of M82 (Marshall *et al.* 1993). It would require five to ten thousand systems emitting at Cyg X-1’s low-state luminosity (several times  $10^{36}$  ergs  $s^{-1}$ ) within a few hundred parsecs of the nucleus to account for the hard X-ray luminosity of M82. Of course, Cyg X-1’s properties may not represent the class; a typical system may in fact be more luminous, requiring fewer such binaries to produce M82’s luminosity. On the other hand, very few black-hole binaries have been identified *anywhere* in the universe; our understanding of their formation rate and lifetime is terribly poor (Cowley 1992) and, at present, we do not know for certain that there are *any* black-hole binaries in M82.

#### 4.1.4. Inverse-Compton Scattered Emission?

Rieke *et al.* (1980) discussed the potential importance of inverse-Compton (IC) scattering to the total X-ray emission from M82. In this scenario, the copious flux of infrared photons associated with the starburst scatters off supernova-generated relativistic electrons. The necessary elements for IC scattering are certainly present in M82. However, Watson *et al.* (1984) dismissed IC scattering as the dominant process based on differences between the radio morphology, which locates the relativistic electron population, and the soft X-ray morphology. But as the PSPC hardness map (Fig. 5) indicates, the *hard* X-ray morphology *is* consistent with the radio morphology. Schaaf *et al.* (1989) exhumed the IC hypothesis to explain the hardness of the 1.4–8.9 keV *EXOSAT* spectrum of M82. Although Seaquist & Odegard (1991) showed that the IC process contributes very little to the X-ray emission in M82’s halo, they concluded that IC losses dominate the cooling of the relativistic electrons in the galaxy’s nuclear region.

Accurate measurement of the hard X-ray spectrum of M82 permits more detailed investigation into the role IC scattering may play. Nonthermal radio and X-ray emission arising from a common population of relativistic electrons with a power law distribution of energies should have power law spectra with the same energy index  $\alpha$  ( $= \Gamma - 1$ ). The orientation, shape, and size ( $\sim 40'' \times 80''$ ) of the region in M82 where the 6–20 cm radio spectral index is 0.7 or less (see Fig. 1 of Seaquist & Odegard 1991) are nearly *identical* to that of the hard X-ray region on the PSPC hardness map ( $\sim 45'' \times 70''$ ), where the X-ray spectrum also has an energy index of 0.7. (The resolution of 6–20 cm spectral index map and the PSPC hardness map are about the same.) Furthermore, our measurement of the intrinsic luminosity of the power law component in the 1.4–8.9 keV band of  $2.5 \times 10^{40}$  ergs  $s^{-1}$  is in excellent agreement with the expected IC luminosity of  $1.2$ – $1.5 \times 10^{40}$  ergs  $s^{-1}$  calculated by Schaaf *et al.* (1989). Taking the size of the IC-emitting region to be  $45''$ – $60''$  (suggested by the hardness map) rather than  $30''$ , as Schaaf *et al.* assumed, brings the agreement between the observed luminosity and the expected IC luminosity even closer. Since the IC emissivity depends on the product of the electron and IR photon energy densities, the

apparent nuclear confinement of M82’s hard X-rays is explained by the rapid decline of both quantities with distance from the nucleus (Seaquist & Odegard 1991).

We conclude that IC scattering is likely to make a significant, if not dominant, contribution to the hard X-ray luminosity of M82. It will require high-resolution images at energies above a few keV, such as those the Advanced X-ray Astrophysics Facility (*AXAF*) will provide, to determine what fraction of the hard X-ray emission is diffuse and what fraction is produced by discrete sources.

#### 4.2. The Spatially Extended X-Ray Emission

The three-component model of M82’s X-ray spectrum indicates the presence of hot gas in M82 emitting at two different characteristic temperatures. The warm 0.5–0.6 keV R-S component is heavily absorbed ( $N_{\text{H}} \approx 10^{22} \text{ cm}^{-2}$ ) and, like the hard X-ray source, must originate in the central region and disk of the galaxy. This component probably arises from an ensemble of supernova remnants, which, individually, can have “warm” spectra with strong emission lines (e.g., Hayashi *et al.* 1994). At high spectral resolution, the emission lines associated with the warm component are poorly fitted with a simple R-S model (§ 3.2). But R-S models often do not accurately describe the spectra of isolated supernova remnants (e.g., Shull 1982; Tsunemi *et al.* 1986), so there is no reason to expect that a simple model should fit the integrated spectrum of a large number of overlapping remnants. The soft 0.3 keV R-S component, which is not absorbed, is likely to represent the extended halo of X-ray emission associated with the starburst-driven “superwind” (Bland & Tully 1988; Heckman, Armus, & Miley 1990). Leitherer, Robert, & Drissen (1992) have estimated that the starburst in M82 injects kinetic energy into the interstellar medium at the rate of  $\sim 6\text{--}30 \times 10^{41} \text{ ergs s}^{-1}$ , well in excess of the combined intrinsic luminosity of the thermal components in our fit ( $1.2 \times 10^{41} \text{ ergs s}^{-1}$ ). For this range of energy injection rates, the superwind model of Suchkov *et al.* (1994) explicitly predicts a total luminosity of  $\sim 10^{41} \text{ ergs s}^{-1}$  for the hot gas and an extended soft X-ray component with  $kT \approx 0.3 \text{ keV}$ —very similar to what we observe. Thus, not only is it energetically feasible for the starburst in M82 to power the observed thermal X-ray emission, the wind generated by the starburst appears to account for the temperature and spatial extent of the emitting gas as well.

### 5. SUMMARY

We have analyzed high signal-to-noise *ROSAT* and *ASCA* X-ray spectra of the starburst galaxy M82 spanning the 0.1–10 keV energy range. At least three spectral components contribute to the total emission from the galaxy, revealing that its high-energy nature is significantly more complex than previous investigations have shown. A consistent model for the broad-band X-ray properties of M82 could not have been determined by analyzing either data set separately.

The observed X-ray flux from M82 is dominated by a strong, hard ( $\Gamma \approx 1.7$ ), heavily absorbed ( $N_{\text{H}} \approx 10^{22} \text{ cm}^{-2}$ ) power law component that originates in the nucleus and near-nuclear disk of the galaxy. While this spectrum resembles that of a typical AGN, there is no other evidence to suggest that M82’s hard X-rays are produced by a buried Seyfert nucleus. A bremsstrahlung model with  $kT \approx 18 \text{ keV}$  provides a good fit to the hard X-ray component, but the strong Fe  $K\alpha$  emission expected to accompany the emission

from gas at this temperature is not observed. The spectra of high- and low-mass X-ray binary systems are not compatible with M82’s spectrum. The Galactic black hole candidate Cyg X-1, however, does have a spectrum similar to that of M82, making it plausible that back-hole binaries are responsible for M82’s hard X-ray emission. But the formation rates and lifetimes of black-hole binaries are tremendously uncertain (Cowley 1992), and the existence of *any* such systems in M82 has yet to be proved. On the other hand, the elements required for inverse-Compton emission—infrared photons and relativistic electrons with the appropriate energy densities—are known to be present in the nuclear region of M82. IC emission, therefore, provides the most straightforward explanation for the production of hard X-rays in M82. We have shown (1) that the intrinsic luminosity of the power-law spectral component agrees closely with the expected inverse-Compton luminosity computed by Schaaf *et al.* (1989), and (2) that the regions in M82 where the radio and X-ray spectra have the same energy index are very similar in location, size, and shape—a necessary condition if the radio and X-ray emission are nonthermal and arise from a common population of relativistic electrons. We conclude, therefore, that the IC process is likely to dominate the emission from M82’s nucleus.

Also contributing to the X-ray emission from M82 are two thermal components with characteristic temperatures of  $\sim 0.5$ – $0.6$  keV and  $\sim 0.3$  keV. The warmer of the two thermal plasmas is also heavily absorbed and may represent supernova remnants and/or a supernova-heated phase of the interstellar medium in the central region of the galaxy. The other thermal component is not absorbed (above the Galactic level) and is likely to represent emission from the starburst-driven wind that extends along M82’s minor axis. Although the latter component contributes just a small fraction of the total X-ray flux, its inclusion in the model is crucial for the determination of a physically plausible picture for the X-ray emission from M82. The thermally emitting gas in M82 may possess a range of properties, despite the fact that it is accurately modeled by components at two distinct temperatures at the resolution of the *ROSAT* PSPC and *ASCA* GIS. The poor fit obtained to the high-resolution *ASCA* SIS spectrum provides a clear indication that the true nature of this gas is considerably more complex. Since the spectra of individual supernova remnants are not always well-fitted by simple R-S models (Shull 1982; Tsunemi *et al.* 1986), it is not surprising that a more sophisticated model is required to fit the spectrum of an ensemble of overlapping supernova remnants.

M82 is frequently regarded as a prototype for starburst galaxies, which gives the *ROSAT* and *ASCA* spectra presented here particular importance. Moreover, they represent the highest signal-to-noise X-ray spectra currently available for such objects. Their analysis, therefore, should assist the interpretation of *ROSAT* and *ASCA* observations of other starbursts. Unfortunately, until data of comparable quality are available for a number of star-forming galaxies, the question of whether or not the X-ray properties of M82 are prototypical remains open.

We are very grateful to David Helfand for a critical reading of the manuscript. This research has made use of *ROSAT* and *ASCA* archival data obtained through the High Energy Astrophysics Science Archive Research Center (HEASARC), provided by NASA Goddard Space Flight Center. Support for this work was provided in part by the U.S. Department of Energy under contract W-7405-ENG-48.

TABLE 1  
PREVIOUS MODELS OF THE INTEGRATED X-RAY SPECTRUM OF M82

Investigator(s)	Instrument	Model <sup>a</sup>	$kT$ (keV) or $\Gamma$	$N_{\text{H}}$ ( $\times 10^{21}$ cm <sup>-2</sup> )
Fabbiano (1988)	<i>Einstein</i> IPC	TB	2.2 ( $> 1.2$ )	$1.7^{+1.7}_{-0.7}$
Fabbiano (1988)	<i>Einstein</i> MPC	TB	$6.8^{+5.7}_{-2.3}$	$< 2.2$
Schaaf et al. (1989)	<i>EXOSAT</i> ME	TB	$9^{+9}_{-4}$	$< 5.5$
		PL	$1.8^{+0.45}_{-0.36}$	$< 10$
Ohashi & Tsuru (1992)	<i>Ginga</i> LAC	TB	$5.8 \pm 0.5$	$13 \pm 7$
Petre (1992)	BBXRT	TB	$6.8 \pm 1.7$	$6 \pm 2$
		<i>plus</i> R-S	0.7	

<sup>a</sup> TB = thermal bremsstrahlung; PL = power law; R-S = Raymond-Smith plasma.

TABLE 2  
 FITS TO THE COMBINED *ROSAT* PSPC/*ASCA* GIS SPECTRUM OF M82

Components In Model	Component	$kT$ (keV) or $\Gamma$	$N_{\text{H}}$ ( $\times 10^{21}$ cm $^{-2}$ )	Model $\chi^2$ ( $\nu$ )
1	PL	1.75	0.87	1631 (450)
1	TB	7.95	0.62	2200 (450)
1	R-S	7.03	0.60	2368 (450)
2	PL	1.58	1.50	579 (445)
	R-S	0.58	0.25	
2	TB	14.7	0.91	595 (445)
	R-S	0.61	0.36	
3	PL	1.70 (1.56–1.90)	17.1 (8.30–27.7)	460 (440)
	R-S	0.52 (0.44–0.68)	10.5 (8.10–12.7)	
	R-S	0.28 (0.22–0.33)	0.46 (0.37–0.60)	
3	TB	18.0 (10.9–33.9)	11.8 (5.70–20.3)	460 (440)
	R-S	0.59 (0.47–0.72)	10.1 (8.20–12.3)	
	R-S	0.29 (0.24–0.34)	0.46 (0.38–0.59)	

NOTE.—90% confidence limits for six interesting parameters are given in parentheses.

TABLE 3  
 FITS TO THE ASCA SIS SPECTRA OF M82

Components In Model	Component	$kT$ (keV) or $\Gamma$	$N_{\text{H}}$ ( $\times 10^{21}$ cm $^{-2}$ )	Model $\chi^2$ ( $\nu$ )
1	PL	1.79	1.04	1852 (271)
2	PL	1.48	1.03	675 (267)
	R-S	0.80	0.65	
3	PL	1.39	7.85	469 (263)
	R-S	0.79	7.77	
	R-S	0.29	0.00	
3	PL	1.70 <sup>a</sup>	13.6	515 (265)
	R-S	0.78	7.78	
	R-S	0.27	0.45 <sup>a</sup>	

<sup>a</sup> Parameter fixed.

REFERENCES

- Bartel, N., *et al.* 1982, *ApJ*, 262, 556  
Bernlöhr, K. 1993, *A&A*, 268, 25  
Bland, J., & Tully, R. B. 1988, *Nature*, 334, 43  
Bregman, J. N., Schulman, E., & Tomisaka, K. 1995, *ApJ*, 439, 155  
Cowley, A. P. 1992, *ARAA*, 30, 287  
Elvis, M., Soltan, A., & Keel, W. 1984, *ApJ*, 283, 479  
Elvis, M., & Van Speybroeck, L. 1982, *ApJ*, 257, L51  
Fabbiano, G. 1988, *ApJ*, 330, 672  
Fabbiano, G. 1989, *ARA&A*, 27, 87  
Hayashi, I., Koyama, K., Ozaki, M., Miyata, E., Tsunemi, H., Hughes, J. P., & Petre, R. 1994, *PASJ*, 46, L121  
Heckman, T. M., Armus, L., & Miley, G. K. 1990, *ApJS*, 74, 833  
Kennicutt, R. C. 1992, *ApJ*, 388, 310  
Koratkar, A., Deusua, S. E., Heckman, T., Filippenko, A. V., Ho, L. C., & Rao, M. 1995, *ApJ*, 440, 132  
Leitherer, C., Robert, C., & Drissen, L. 1992, *ApJ*, 401, 596  
Marshall, F. E., Mushotzky, R. F., Petre, R., & Serlemitsos, P. J. 1993, *ApJ*, 419, 301  
Matsuoka, M., Piro, L., Yamauchi, M., & Murakami, T. 1990, *ApJ*, 361, 440  
Muxlow, T. W. B., Pedlar, A., Wilkinson, P. N., Axon, D. J., Sanders, E. M., & de Bruyn, A. G. 1994, *MNRAS*, 266, 455  
Nagase, F. 1989, *PASJ*, 41, 1  
Nandra, K., & Pounds, K. A. 1994, *MNRAS*, 268, 405  
Peimbert, M., & Torres-Peimbert, S. 1981, *ApJ*, 245, 845  
Petre, R. 1992, in *The Nearest Active Galaxies*, eds. J. Beckman, L. Colina, & H. Netzer (Madrid: CSIC), p. 117  
Puxley, P. J., Brand, W. J. L., Moore, T. J. T., Mountain, C. M., Nakai, M., & Yamashita, T. 1989, *ApJ*, 345, 163.  
Rieke, G. H., Lebofsky, M. J., Thompson, R. I., Low, F. J., & Tokunaga, A. T. 1980, *ApJ*, 238, 24  
Schaaf, R., Pietsch, W., Biermann, P. L., Kronberg, P. P., & Schmutzler, T. 1989, *ApJ*, 336, 722  
Seaquist, E. R., & Odegard, N. 1991, *ApJ*, 369, 320  
Shull, J. M. 1982, *ApJ*, 262, 308  
Stark, A. A., Gammie, C. F., Wilson, R. W., Bally, J., Linke, R. A., Heiles, C., & Hurwitz, M. 1992, *ApJS*, 79, 77  
Suchkov, A. A., Balsara, D. S., Heckman, T. M., & Leitherer, C. 1994, *ApJ*, 430, 511  
Tammann, G. A., & Sandage, A. R. 1968, *ApJ*, 151, 825  
Tsunemi, H., Yamashita, K., Masai, K., Hayakawa, S., & Koyama, K. 1986, *ApJ*, 306, 248  
Watson, M. G., Stanger, V., & Griffiths, R. E. 1984, *ApJ*, 286, 144  
White, N. E., Peacock, A., Hasinger, G., Mason, K. O., Manzo, G., Taylor, G. B., & Branduardi-Raymont, G. 1986, *MNRAS*, 218, 129  
Zombeck, M. V. 1990, *Handbook of Space Astronomy and Astrophysics*, (Cambridge: Cambridge University Press), pp. 103–104

FIGURE CAPTIONS

Fig. 1.—Total 0.1–2.4 keV intensity contours from the *ROSAT* PSPC image of M82, overlaid on an optical image of the galaxy from the POSS E plate. The X-ray image was smoothed using a Gaussian with  $\sigma = 10''$ . Contours at the 2, 5, 10, 20, 40, 120, and 240  $\sigma$  levels are plotted.

Fig. 2.—The observed *ROSAT* PSPC (left) and *ASCA* GIS (right) spectra of M82, with the best-fit (a) two-component and (b) three-component models from Table 2 (folded through the instrument response functions). For these plots, the spectra have been rebinned so that the signal-to-noise ratio in each channel is at least 12. A power law was used for the hard component.

Fig. 3.—The PSPC (left) and GIS3 (right) spectra of M82 and the best-fit three-component model (with the instrument response functions unfolded) illustrate the relative contribution of each component to the total X-ray emission from M82. The hard, warm, and soft components, and their sum, are indicated with dashed, dot-dashed, dotted, and solid lines, respectively. At energies less than  $\sim 0.6$  keV, the soft thermal component accounts for virtually all of the flux, whereas at energies greater than  $\sim 1.3$  keV, the flux is dominated by the hard component. A power law was used for the hard component in this plot.

Fig. 4.—Detail of the SIS0 and SIS1 spectra of M82 in the 0.7–2.4 keV range. The spectra are fitted with the fourth model listed in Table 3. The fit residuals indicate that the model, while fitting some of the emission lines well (e.g., the Mg XII and Si XIII lines at 1.47 and 1.87 keV), misses badly in other cases (e.g., the Ne IX, Mg XI, and Si XIV lines at 0.92, 1.34, and 2.01 keV).

Fig. 5.—The X-ray “hardness map” of M82 (grey scale), made from the ratio of smoothed ( $\sigma = 10''$ ) hard-band ( $> 1$  keV) and soft-band ( $< 1$  keV) *ROSAT* PSPC images. The 0.1–2.4 keV intensity contours, identical to those shown in Fig. 1, are overlaid. The hard-to-soft counts ratios in the (black) nuclear region, which measures  $\sim 45'' \times 70''$ , range from  $\sim 2$  to 4. The halo emission extending along M82’s minor axis is comparatively much softer, with hard-to-soft counts ratios of 0.2–0.4. The axes are labeled with J2000 coordinates.

Fig. 6.—Background-subtracted GIS2 + GIS3 light curve in the 3.5–10 keV band, which isolates M82’s nuclear X-ray emission. In the top panel, the data have been binned at 256 s intervals. Data from an entire orbit have been binned together in the lower panel. The mean count rate is indicated with dotted lines. Light curves for the background are displayed at the bottom of each panel. No significant variations on timescales of minutes or hours are observed.

Fig. 7.—Optical spectrum of M82’s nucleus near  $H\alpha$   $\lambda 6563$ , obtained from three 30 minute observations with the Kitt Peak 4 m telescope under photometric conditions. A fit to the stellar continuum has been subtracted. A broad Gaussian line with a flux of  $6 \times 10^{-15}$  ergs  $\text{cm}^{-2} \text{s}^{-1}$  and a width of  $3000 \text{ km s}^{-1}$  has been overlaid at the wavelength of  $H\alpha$ . Such a line would be expected if a Seyfert nucleus was responsible for M82’s hard X-ray emission. The vertical axis has units of ergs  $\text{cm}^{-2} \text{s}^{-1} \text{\AA}^{-1}$ .

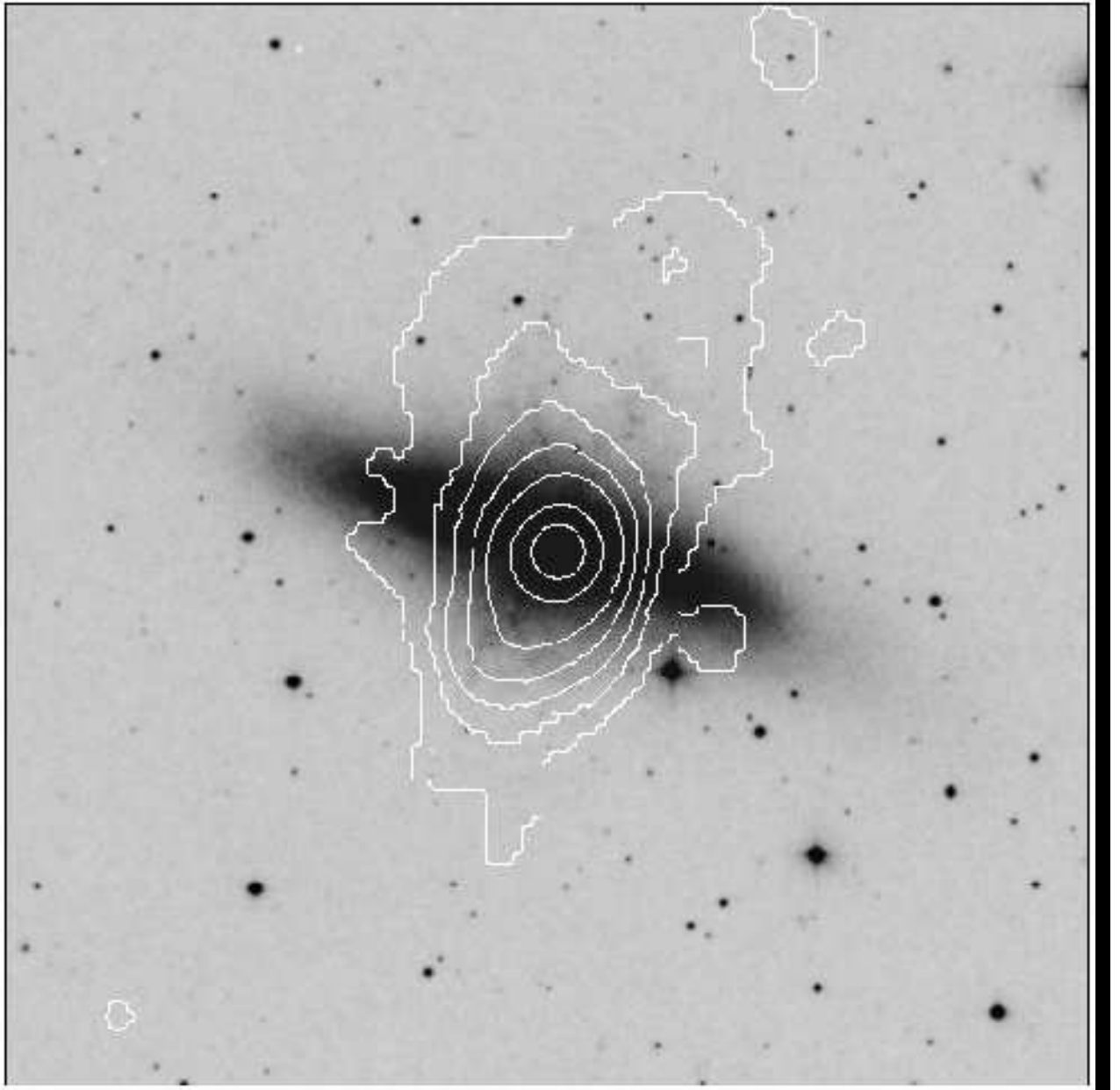


Figure 1

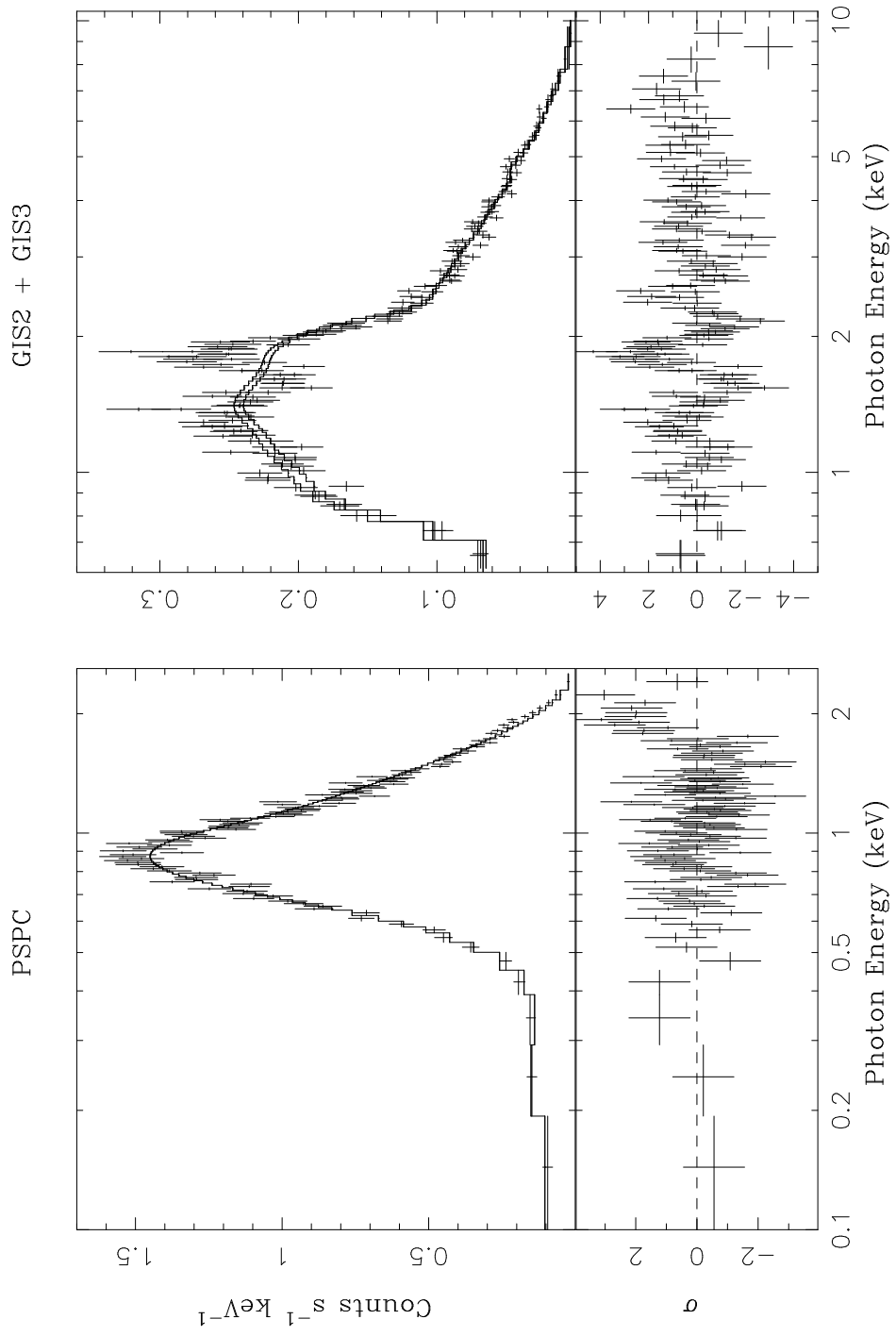


Figure 2a

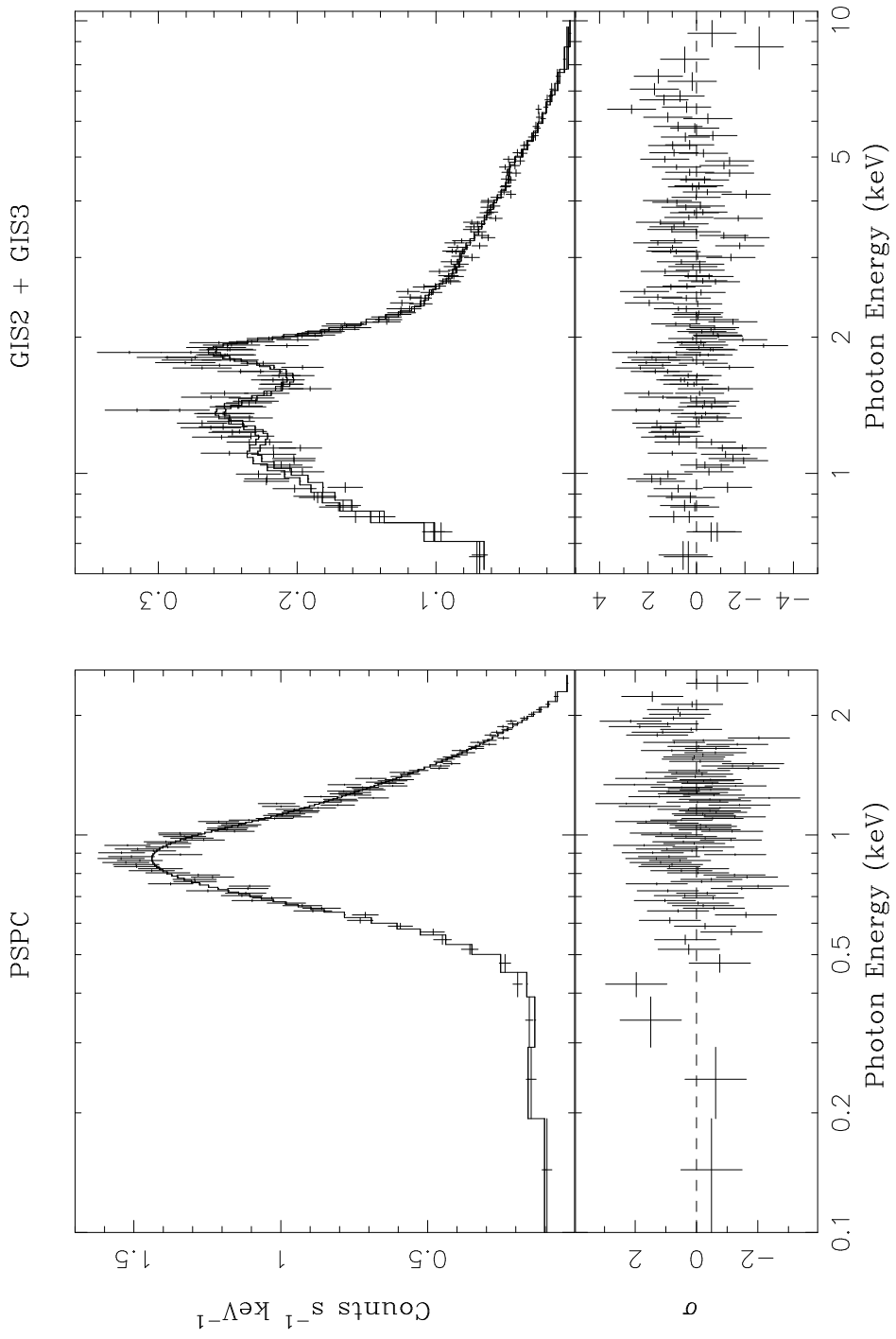


Figure 2b

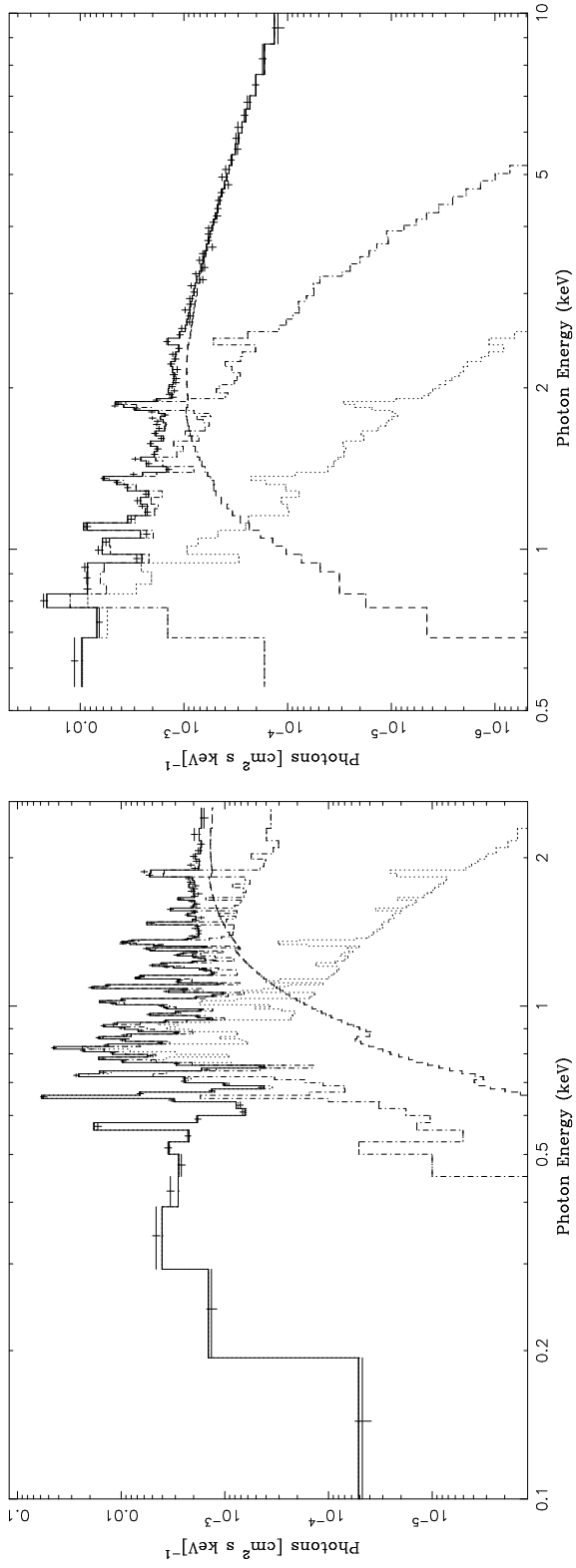


Figure 3

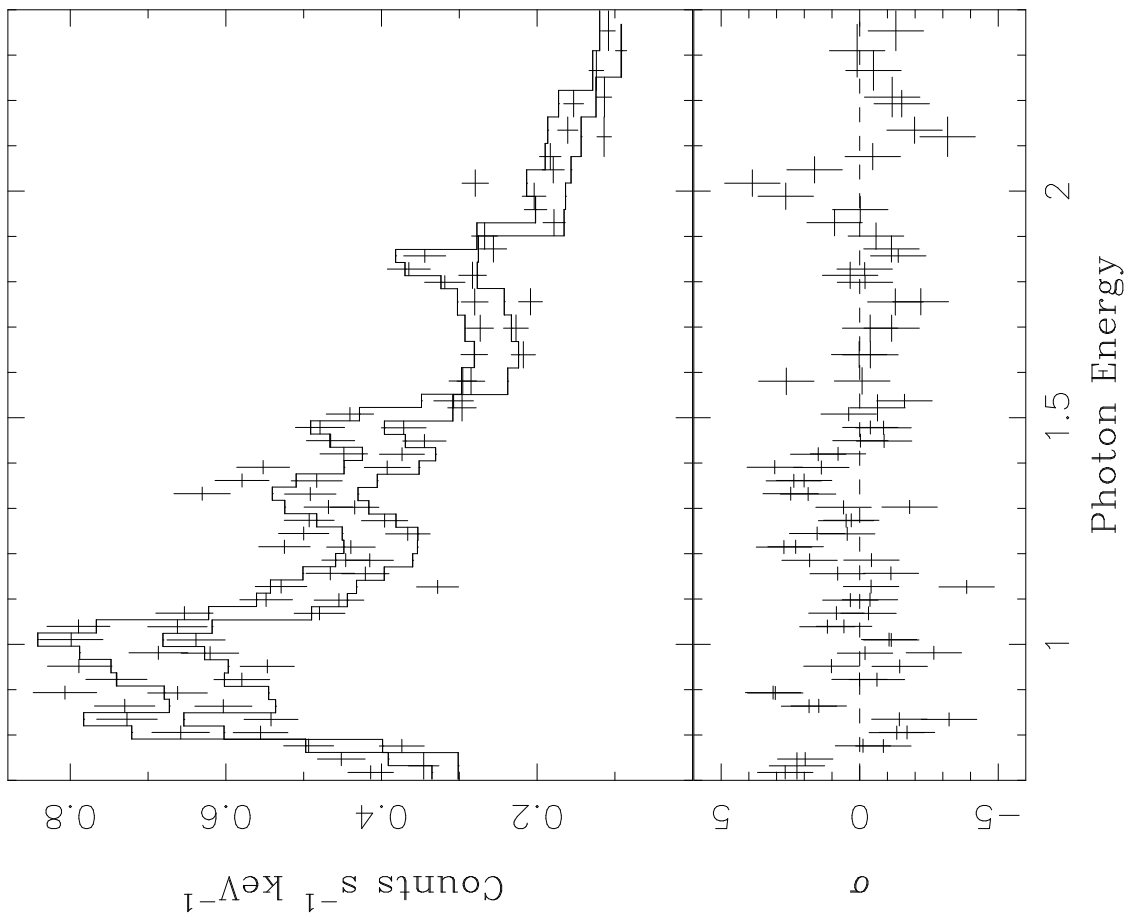


Figure 4

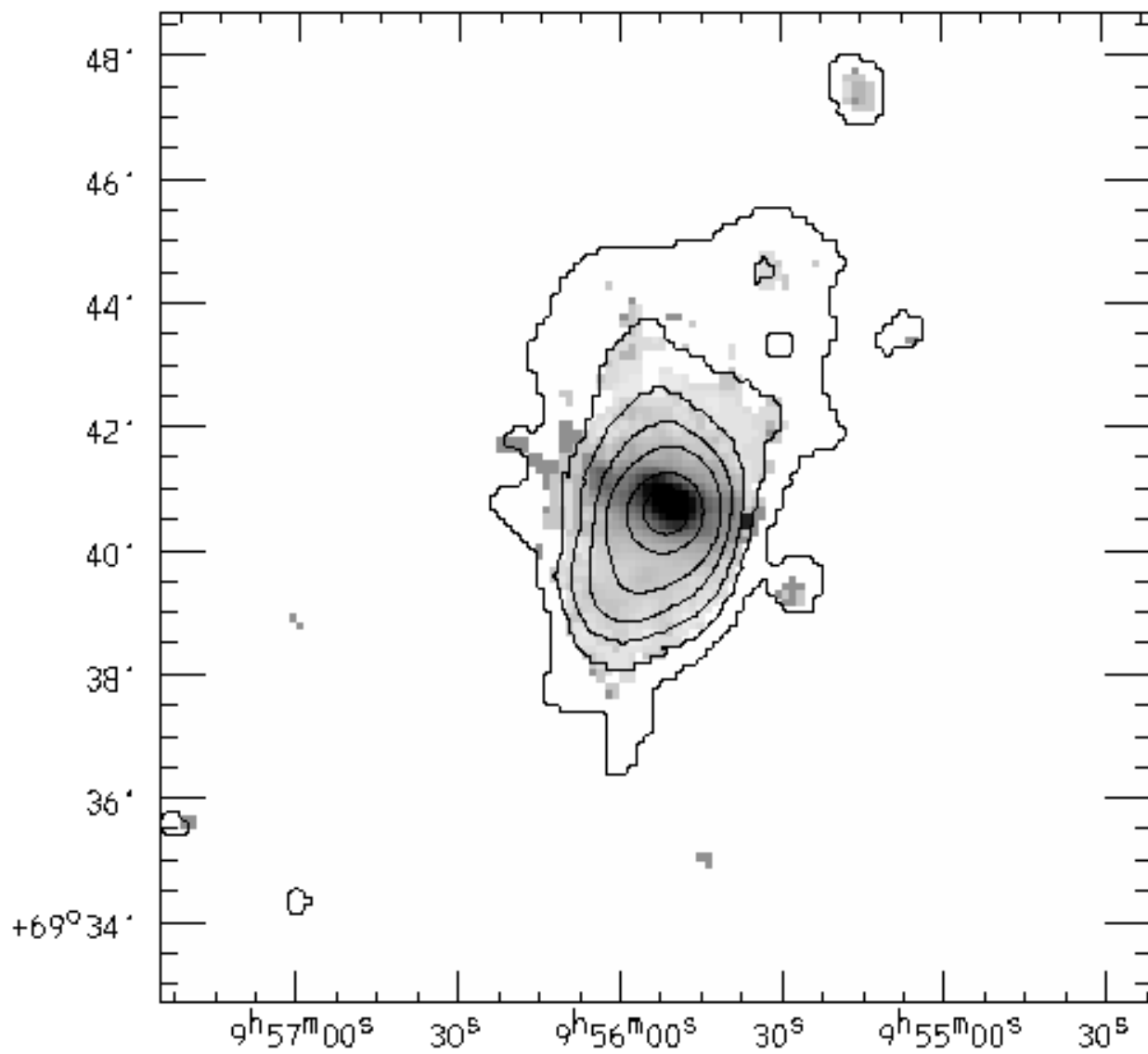


Figure 5

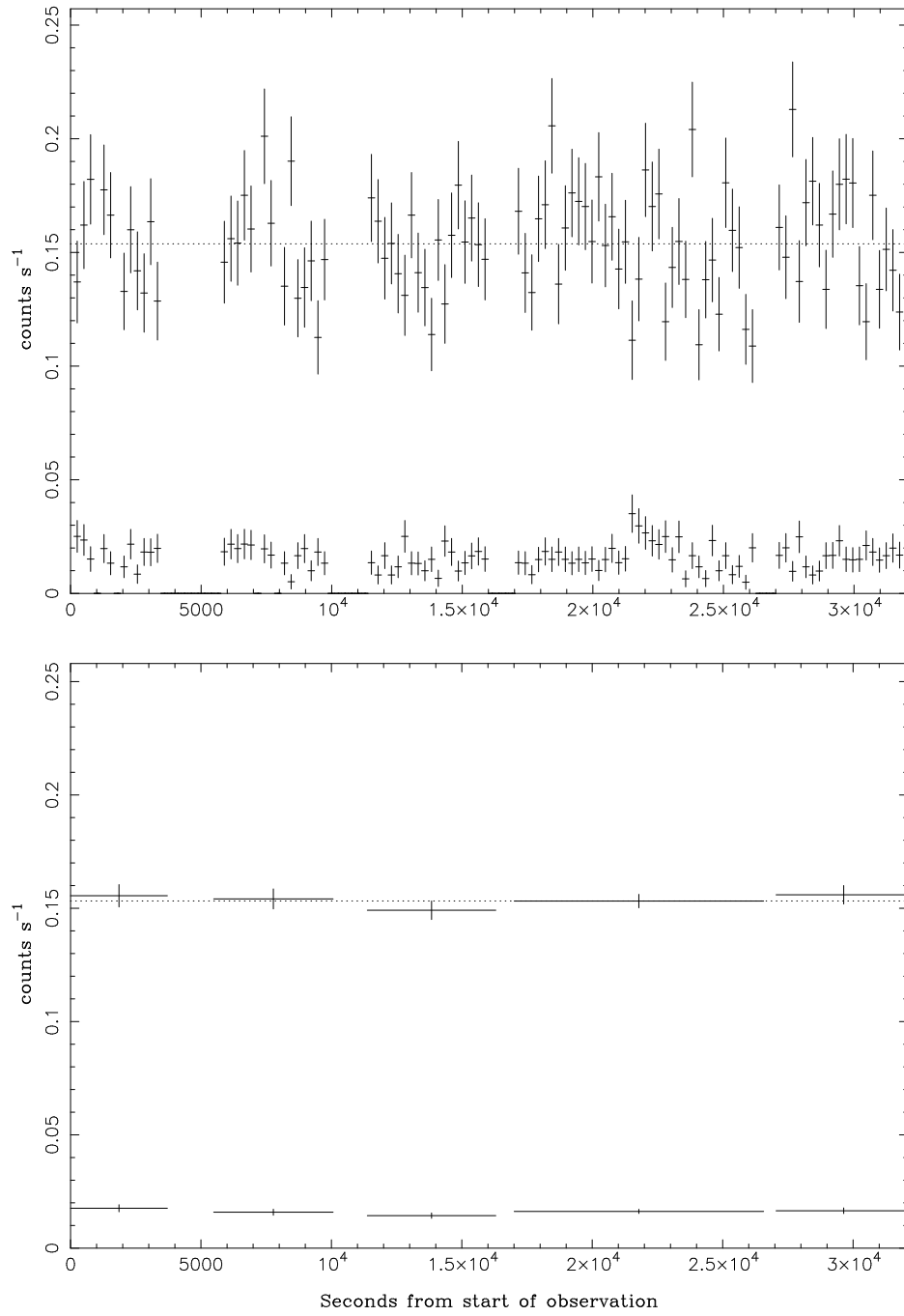


Figure 6

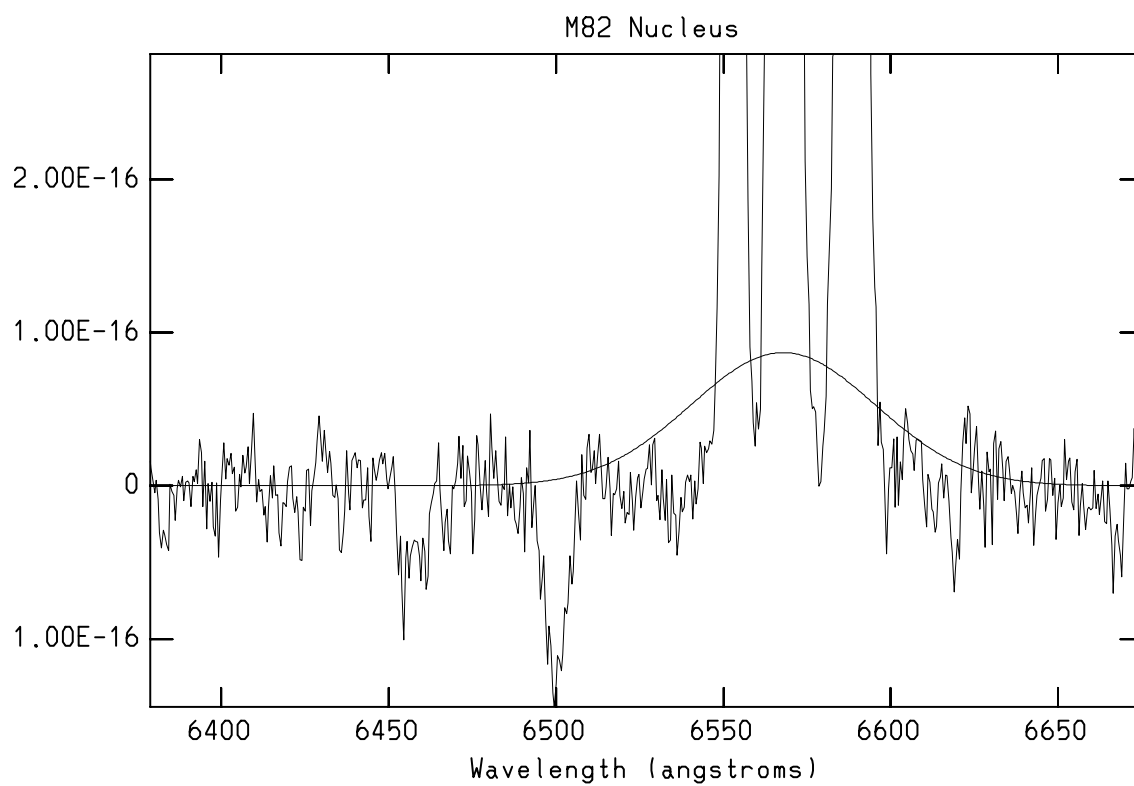


Figure 7